A Two-User Successive Interference Cancellation LoRa Receiver with Soft-Decoding

Mathieu Xhonneux[†], Joachim Tapparel[*], Péter Scheepers[‡], Orion Afisiadis[*], Alexios Balatsoukas-Stimming[‡], David Bol[†], Jérôme Louveaux[†], and Andreas Burg[*]
[*]Telecommunication Circuits Laboratory, EPFL, Switzerland
[†]ICTEAM, UCLouvain, Belgium
[‡]Department of Electrical Engineering, Eindhoven University of Technology, The Netherlands

***Abstract*—LoRaWAN is a popular wireless technology that provides long-range connectivity to Internet-of-Things devices using a bit-interleaved coded modulation. To minimize their energy consumption, LoRaWAN end-nodes implement a pure ALOHA access scheme, which leads to collisions among users at the gateway and a reduced throughput in crowded networks. To improve the throughput of interference-limited LoRaWAN networks, we design in this paper a successive interference cancellation receiver that is able to decode frames from two colliding users with the same spreading factor. By performing both a soft-demodulation and soft-decoding to recover the message of each interfering user, the proposed two-user receiver explicitly leverages the coded spread spectrum modulation of LoRa. We show that the joint usage of interleaving and coding is critical to achieve a decent cancellation of the strongest user. Simulation results indicate that our receiver successfully demodulates the frames of two interfering users with a 1.5 dB difference of received powers, even at very low signal-to-noise ratios.**

I. Introduction

With the rise of the Internet of Things (IoT), LoRaWAN has become the leading wireless technology to connect ultra low-power smart end-nodes. Unlike 3GPP cellular standards such as NB-IoT, LoRaWAN uses low-complexity PHY and MAC layers to minimize the energy overhead of IoT communications. Its PHY layer, usually named LoRa, uses a chirp spread spectrum (CSS) modulation combined with Hamming codes in a bit-interleaved coded modulation (BICM) scheme [1], [2]. This particular combination of a spread spectrum modulation and coding enables receivers to attain sensitivities as low as -130 dBm. In reception, the CSS modulation provides an important spreading gain, which is determined by the spreading factor (SF). The SF defines the length of a LoRa symbol, and allows to trade off transmission time and data rate for coverage.

At the MAC layer, LoRaWAN implements a pure ALOHA multiple access scheme. Since the end-nodes are not synchronized, interference between users that share the same channel is the main source of errors in dense networks [3], [4]. We distinguish two types of interference in LoRaWAN networks: *inter-SF interference* and *same-SF interference*. LoRa transmissions using different SFs can be seen as near-orthogonal [5], whereas simultaneous transmissions with the same SF behave as destructive interference. In particular, same-SF colliding LoRa packets undergo a *capture effect*, such that the strongest signal can often be demodulated at the expense of the weakest signal as long as the signal-to-noise ratio (SNR) and signal-to-interference ratio (SIR) are sufficiently high [6].

To date, two main approaches have been followed in the literature to improve the throughput of interference-limited LoRaWAN networks. Some works extend the underlying ALOHA multiple access of LoRaWAN by synchronizing the end-nodes in time and framing their transmissions in time slots to avoid collisions [7]–[9]. These solutions however incur a significant energy overhead as the end-nodes need to listen to beacons from the gateway to maintain their synchronization in time. The second approach consists of decoding colliding same-SF transmissions using multi-user receivers [10]–[13]. Such receivers allow to increase the throughput of a pure ALOHA network [14], without requiring any modifications at the MAC layer. However, designing LoRa multi-user receivers capable of demodulating two colliding packets at the low SNR levels (-25 dB to -5 dB) at which LoRa commonly operates is a challenging problem. The different receivers proposed so far in the literature do not exhibit useful error rates at practical SNRs.

Contributions: We propose a two-user LoRa successive interference cancellation (SIC) receiver capable of demodulating two colliding users with the same SF. This SIC receiver decodes the message of the user with the greatest power, and then cancels its contribution from the received signal in order to decode the remaining user. Contrary to other LoRa SIC receivers in the literature (e.g., [10]), our receiver performs a soft-demodulation and soft-decoding of both users. The soft-information obtained from decoding the strongest user is leveraged to reconstruct its signal in the SIC algorithm. Thanks to the interleaving and the coding of the BICM scheme, we show that our proposed two-user receiver attains useful error rates in the targeted SNR regime.

II. The LoRa Physical Layer

In this section, we provide a brief explanation of the LoRa physical layer. We first explain how LoRa implements BICM with its particular chirp spread spectrum modulation and we subsequently explain how a conventional single-user LoRa receiver performs soft-demodulation and soft-decoding of the received symbols. In preparation for the next section, we then extend the single-user signal model to include two interfering LoRa users employing the same spreading factor.

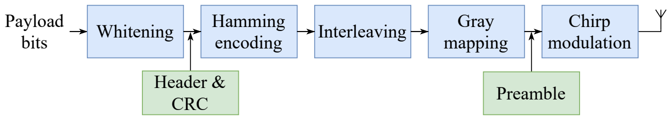

Fig. 1: Illustration of the LoRa PHY Tx chain, which implements Bit-Interleaved Coded Modulation.

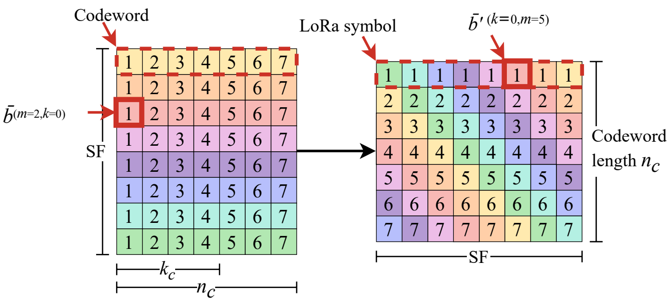

Fig. 2: LoRa interleaving for $\mathrm{SF} = 8$ and a $(4, 7)$ Hamming code.

A. The LoRa Tx Chain

To enable energy-efficient long range communications, LoRa uses a spread spectrum modulation with $N = 2^{\mathrm{SF}}$ orthogonal waveforms [15], where $\mathrm{SF} \in \{7, \ldots, 12\}$ is called the *spreading factor*. The waveforms are chirps, i.e., complex phasors whose instantaneous frequency increases linearly over time and spans a bandwidth $B \in \{125, 250, 500\}$ kHz. Each waveform consists of N samples when sampled at the frequency $f_s = B$ and encodes SF bits of information. Increasing the spreading factor SF increases the spreading gain of the modulation, and thus the communication range, but at the expense of decreasing the data rate. A symbol $s \in \{0, \ldots, N-1\}$ is modulated to the discrete-time baseband-equivalent signal $x_s[n]$ by selecting the initial frequency of the chirp [15], [16]

$$x_s[n] = \begin{cases} e^{j2\pi\left(\frac{n^2}{2N}\left(\frac{B}{f_s}\right)^2 + \left(\frac{s}{N} - \frac{1}{2}\right)\left(\frac{B}{f_s}\right)n\right)}, & 0 \leq n < n_f, \\ e^{j2\pi\left(\frac{n^2}{2N}\left(\frac{B}{f_s}\right)^2 + \left(\frac{s}{N} - \frac{3}{2}\right)\left(\frac{B}{f_s}\right)n\right)}, & n_f \leq n < N, \end{cases} \tag{1}$$

where $n_f = N - s$ is the sample index at which a frequency step of $-B$ occurs such that the modulated signal remains in the allocated bandwidth.

To improve its robustness against noise, interference, and residual time and frequency offsets, LoRa combines the chirp spread spectrum modulation with an error correcting code using BICM [17]. A LoRa transmitter, illustrated in Fig. 1, consists of the serial concatenation of a Hamming encoder with the N-dimensional memoryless chirp modulation through a bit interleaver and a one-to-one binary Gray labeling [2], [16]. Conventional (k_c, n_c) Hamming codes with $k_c = 4$ and $n_c \in \{5, 6, 7, 8\}$ are used, where k_c denotes the data word length and n_c denotes the codeword length. The interleaving stage is a simple block diagonal interleaver with the arrangement shown in Fig. 2. The Gray labeling then maps groups of SF bits into symbols $s \in \{0, \ldots, N-1\}$.

Apart from the previously mentioned blocks, the Tx chain also includes a whitening block, the addition of a header and a cyclic redundancy check (CRC) to the whitened payload bits, and the concatenation of a preamble before the modulated symbols. The whitening is a simple XOR operation with a known pseudo-random sequence and has no effect on the performance. We hence ignore the whitening in the remainder of this paper.

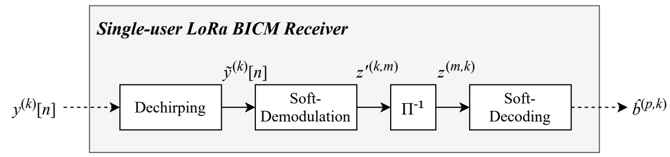

Fig. 3: Illustration of a single-user BICM LoRa soft-receiver.

B. Detection and Decoding for LoRa

Commercial single-user LoRa receivers use a soft-input soft-output (SISO) demodulator and a SISO decoder to properly benefit from the BICM scheme [1], [18]. The architecture of such a single-user LoRa receiver is shown in Fig. 3. To describe its functioning, we now consider only one user transmitting a sequence of $k_c\mathrm{SF}$ payload bits over an AWGN channel. As annotated in Fig. 2, we denote the transmitted payload bits as $b^{(m,p)}$ with $m \in \{0, \ldots, \mathrm{SF}-1\}$ and $p \in \{0, \ldots, k_c - 1\}$ denoting the row and column, respectively, of the bit matrix before encoding and interleaving. Further, let $\bar{b}^{(m,k)}$ and $\bar{b}'^{(k,m)}$ with $k \in \{0, \ldots, n_c - 1\}$ be the corresponding coded bits before and after interleaving, respectively. The n_c rows of bits $\bar{b}'^{(k,m)}$ are mapped to the symbols $x^{(k)}[n]$ using (1).

The corresponding n_c received LoRa symbols are represented by $y^{(k)}[n] = h^{(k)} x^{(k)}[n] + w^{(k)}[n]$, where $n \in \{0, \ldots, N-1\}$, $w^{(k)}[n] \sim \mathcal{CN}(0, \sigma^2)$ is complex AWGN with variance σ^2 and $h^{(k)} \in \mathbb{C}$ is the complex-valued channel gain during the transmission of the k-th symbol. In this paper, we assume that the magnitudes of the gains $h^{(k)}$ are constant and equal to $\sqrt{P}$ during the whole packet reception, whereas the phase of $h^{(k)}$ may slowly change over time due to limited accuracy of the low-cost crystals embedded in IoT end-nodes [19]. We hence define for each received symbol a different initial phase $\theta^{(k)} = \angle h^{(k)}$.

LoRa receivers typically perform a non-coherent detection of the received symbols to avoid the tracking of the phase $\theta^{(k)}$ [16]. For this kind of detection, the likelihood that the transmitter sent the candidate symbol $\bar{s}$ during the k-th window is given by [20]

$$\Lambda(\bar{s}|y^{(k)}) = C \cdot I_0\left(\frac{\sqrt{P}}{\sigma^2}\left|\sum_{n=0}^{N-1} y[n] e^{-j2\pi\left(\frac{n^2}{2N} + n\left(\frac{\bar{s}}{N} - \frac{1}{2}\right)\right)}\right|\right), \tag{2}$$

where $I_0(x)$ is the first order modified Bessel function of the first kind and C is a constant common to all symbols. To allow a more intuitive understanding of (2), an intermediate *dechirping* stage is often introduced in the receiver. This stage performs a pointwise multiplication of the received signal with $x_0^*[n]$, the complex conjugate of an unmodulated symbol: $\tilde{y}^{(k)}[n] = y^{(k)}[n] \cdot x_0^*[n] = h^{(k)} e^{j2\pi \frac{s^{(k)} n}{N}} + \tilde{w}^{(k)}[n]$, where

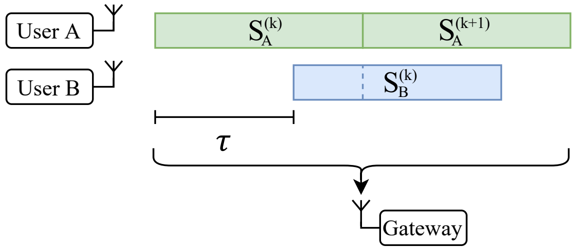

Fig. 4: Illustration of the asynchronicity in time between the users A and B, with the sampling time offset τ.

$\tilde{w}^{(k)}[n] = w^{(k)}[n] \cdot x_0^*[n]$. The summation in (2) then becomes a discrete Fourier transform (DFT) of the dechirped signal

$$\Lambda(\bar{s}|y^{(k)}) = C \cdot I_0 \left(\frac{\sqrt{P}}{\sigma^2} \left| Y^{(k)}[\bar{s}] \right| \right), \tag{3}$$

where $Y^{(k)}[\bar{s}]$ is the N-point DFT of $\tilde{y}^{(k)}[n]$.

To compute soft information at the output of the demodulator, the likelihoods $\Lambda(\bar{s}|y^{(k)})$ are mapped to log-likelihood ratios (LLRs) [21]

$$z'^{(k,m)} = \log \frac{\sum_{\bar{s}: g_m(\bar{s})=1} \Lambda(\bar{s}|y^{(k)})}{\sum_{\bar{s}: g_m(\bar{s})=0} \Lambda(\bar{s}|y^{(k)})}, \tag{4}$$

where $g_i(\bar{s})$ returns the i-th bit of the symbol $\bar{s}$ in the Gray labeling. In practical receivers, the complexity of computing the LLRs $z'^{(k,m)}$ is reduced by using the max-log approximation [22], which here yields

$$\begin{aligned} z'^{(k,m)} = &\max_{\bar{s}: g_m(\bar{s})=1} \left[\log I_0 \left(\frac{\sqrt{P}}{\sigma^2} \left| Y[\bar{s}] \right| \right) \right] \\ &- \max_{\bar{s}: g_m(\bar{s})=0} \left[\log I_0 \left(\frac{\sqrt{P}}{\sigma^2} \left| Y[\bar{s}] \right| \right) \right]. \end{aligned} \tag{5}$$

The LLRs $z'^{(k,m)}$ are subsequently de-interleaved. The output $z^{(m,k)}$ of the de-interleaver is fed to a Hamming soft-decoder (e.g., [23]). This soft-decoder outputs new LLR values $v^{(m,k)}$, from which an estimation $\hat{b}^{(m,p)}$ of the transmitted bits is obtained.

C. Signal Model for Two Interfering Users

We now extend the model to two superimposed users with the same SF, namely user A and user B. This model has previously been derived in [13] and is the basis for the construction of the two-user detector in Section III. Let us define $s_{\mathrm{A}}^{(k)}$ and $s_{\mathrm{B}}^{(k)}$ as the k-th colliding symbols sent by users A and B, respectively. The symbols $s_{\mathrm{A}}^{(1)}$ and $s_{\mathrm{B}}^{(1)}$ are hence the two first information symbols of both users that collide with each other. Due to the non-slotted ALOHA multiple access scheme, the users are not synchronized to each other in time. We define $\tau \in [0, N)$ as the relative sample-level time offset between the first sample of the first colliding symbol transmitted by user A and the first sample of the first colliding symbol of user B, as illustrated in Fig. 4. This offset can be split into an integer part $L_{\text{STO}} = \lceil \tau \rceil$ and a non-integer part $\lambda_{\text{STO}} = \tau - \lceil \tau \rceil$ [6]. In order to simplify the notation of the model, we also assume that the gateway is synchronized in both frequency and time to user A.

Since the transmission of user B experiences an STO $\tau \geq 0$ with respect to user A, the first $\lceil \tau \rceil$ samples of symbol $s_{\mathrm{A}}^{(k)}$ overlap with symbol $s_{\mathrm{B}}^{(k-1)}$ and the last $N - \lceil \tau \rceil$ samples of symbol $s_{\mathrm{A}}^{(k)}$ overlap with symbol $s_{\mathrm{B}}^{(k)}$. The contribution of user B to the k-th window of N samples $y^{(k)}[n]$ can therefore be split into two parts, namely $y_{\mathrm{B},1}^{(k)}[n]$ for $n \in \mathcal{N}_1 = \{0, \ldots, \lceil \tau \rceil - 1\}$ and $y_{\mathrm{B},2}^{(k)}[n]$ for $n \in \mathcal{N}_2 = \{\lceil \tau \rceil, \ldots, N-1\}$, with

$$y_{\mathrm{B},1}^{(k)}[n] = e^{j2\pi \left(\frac{(n+N-\tau)^2}{2N} + (n+N-\tau) \left(\frac{s_{\mathrm{B}}^{(k-1)}}{N} - \frac{1}{2} - u\left[n - n_{f,1}^{(k)}\right] \right) \right)},$$

$$y_{\mathrm{B},2}^{(k)}[n] = e^{j2\pi \left(\frac{(n-\tau)^2}{2N} + (n-\tau) \left(\frac{s_{\mathrm{B}}^{(k)}}{N} - \frac{1}{2} - u\left[n - n_{f,2}^{(k)}\right] \right) \right)},$$

and $n_{f,1}^{(k)} = \lceil \tau \rceil - s_{\mathrm{B}}^{(k-1)}$, $n_{f,2}^{(k)} = N + \lceil \tau \rceil - s_{\mathrm{B}}^{(k)}$ [13], [24].

Prior to synchronization, both users are affected by distinct carrier frequency offsets relative to the receiver, namely $\Delta f_{c,\mathrm{A}}$ and $\Delta f_{c,\mathrm{B}}$. However, since we assume that the receiver is synchronized to user A, there is a single residual CFO $\Delta f_c = \Delta f_{c,\mathrm{B}} - \Delta f_{c,\mathrm{A}}$ that only affects the signal from user B. Also, let P_{A} and P_{B} be the received powers of users A and B, respectively. As previously explained, we do not make any assumption on the phase coherence of successive symbols, and thus define $\theta_{\mathrm{A}}^{(k)}$ and $\theta_{\mathrm{B}}^{(k)}$ as the initial independent phases of the corresponding symbols of user A and B, respectively. The baseband-equivalent model of the sampled signal contained in the k-th window of N samples is therefore

$$\begin{aligned} y^{(k)}[n] = &\sqrt{P_{\mathrm{A}}} e^{j\theta_{\mathrm{A}}^{(k)}} x_{s_{\mathrm{A}}^{(k)}}[n] + w^{(k)}[n] \\ &+ \begin{cases} \sqrt{P_{\mathrm{B}}} e^{j\theta_{\mathrm{B}}^{(k-1)}} c[n] y_{\mathrm{B},1}^{(k)}[n], & n \in \mathcal{N}_1, \\ \sqrt{P_{\mathrm{B}}} e^{j\theta_{\mathrm{B}}^{(k)}} c[n] y_{\mathrm{B},2}^{(k)}[n], & n \in \mathcal{N}_2, \end{cases} \end{aligned} \tag{6}$$

where $c[n] = e^{j2\pi n \frac{\Delta f_c}{f_s}}$ is the residual CFO affecting user B.

III. A Two-User Successive Interference Cancellation LoRa Soft-Detector

Based on the previously described single-user detector, we now design a two-user LoRa SIC soft-detector. This detector demodulates simultaneously two interfering users that overlap in time with the same SF. The strongest user is first decoded and its contribution to the received signal is removed before the weakest user is decoded. Since LoRa uses an orthogonal symbol alphabet, the usage of conventional soft-interference cancellation schemes is not straightforward. Our proposed two-user detector performs instead a hard interference cancellation of the strongest user, which still leverage the soft-output of the Hamming decoding.

In a practical gateway, an instance of this detector should be deployed for each SF, since users with different SFs can be demodulated in parallel without interfering significantly with each other. Since we have already demonstrated in a previous paper that two-user synchronization can easily be achieved [13], we assume for the remainder of this paper that the proposed two-user detector is always synchronized to the

$$\tilde{y}^{(k)}[n] = \begin{cases} \sqrt{P_{\text{A}}} e^{j\theta_{\text{A}}^{(k)}} e^{j2\pi\frac{n}{N}s_{\text{A}}^{(k)}} + \sqrt{P_{\text{B}}} e^{j\theta_{\text{B}}^{(k-1)} + 2\pi\tau u\left[n - n_{f,1}^{(k)}\right]} e^{j2\pi\frac{n}{N}\left(s_{\text{B}}^{(k-1)} - \tau + N\frac{\Delta f_c}{f_s}\right)} + \tilde{w}^{(k)}[n], & n \in \mathcal{N}_1, \\ \sqrt{P_{\text{A}}} e^{j\theta_{\text{A}}^{(k)}} e^{j2\pi\frac{n}{N}s_{\text{A}}^{(k)}} + \sqrt{P_{\text{B}}} e^{j\theta_{\text{B}}^{(k)} + 2\pi\tau u\left[n - n_{f,2}^{(k)}\right]} e^{j2\pi\frac{n}{N}\left(s_{\text{B}}^{(k)} - \tau + N\frac{\Delta f_c}{f_s}\right)} + \tilde{w}^{(k)}[n], & n \in \mathcal{N}_2. \end{cases} \tag{7}$$

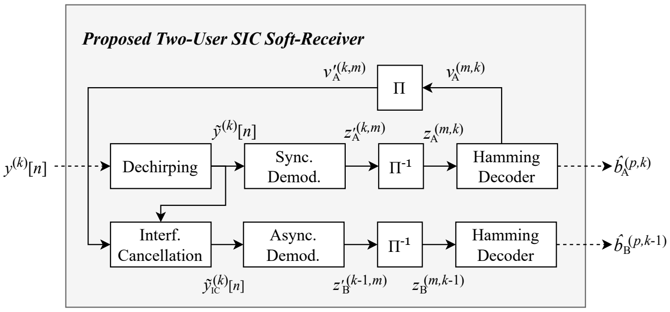

Fig. 5: Illustration of the proposed two-user SIC soft-receiver.

strongest user and that it has perfect knowledge of the users received powers P_{A} and P_{B}, and of the STO τ and the residual CFO Δf_c between them.

A. Architecture of the Proposed Detector

Fig. 5 shows the architecture of the proposed SIC two-user soft-detector. The baseband signal $y^{(k)}[n]$ is retrieved using a single receiving antenna and radio-frequency front-end. The detector contains two branches, each detecting a different user. The upper branch performs first the soft-demodulation and detection of the user with the strongest received power. In the lower branch, the presumed signal contribution of the strongest user is subtracted from the received signal and the message of the weakest user is decoded. If only one user alone is detected by the synchronization stage, only the upper branch is used and the proposed detector falls back to the single-user soft-detector presented in Section II.

In the following derivations, we assume without loss of generality that $P_{\text{A}} > P_{\text{B}}$. The gateway is hence synchronized to user A. The received samples after synchronization are split into windows $y^{(k)}[n]$ of N samples, following the signal model from (6). The detector first dechirps each window of N samples, yielding the dechirped signal $\tilde{y}^{(k)}[n]$ whose expression is provided in (7). The operations used to detect the strongest user are identical to those of the single-user detector presented in Section II. The soft-demodulator of (5) processes the dechirped signal $\tilde{y}^{(k)}[n]$ with $\sqrt{P} = \sqrt{P_{\text{A}}}$ and by considering the contribution of user B only as additional white noise. The LLRs $z'^{(k,m)}_{\text{A}}$ from the demodulator are then de-interleaved and fed to the SISO Hamming decoder from [23], which yields in return the soft-output $v^{(m,k)}_{\text{A}}$. The bits of user A are subsequently estimated by retrieving the signs of the LLRs $v^{(m,k)}_{\text{A}}$.

After the decoding of user A, the interleaved LLRs $v'^{(k,m)}_{\text{A}}$ are used by an interference cancellation algorithm to estimate and subtract the contribution of this user from the dechirped signal $\tilde{y}^{(k)}[n]$, as detailed in the following subsection. Let $\tilde{y}^{(k)}_{\text{IC}}[n]$ be the interference-cancelled signal. Due to the STO τ, each window $\tilde{y}^{(k)}_{\text{IC}}[n]$ contains two symbols of user B. The demodulation of the k-th symbol of user B hence requires specific matched filters that account for the STO τ on the windows $\tilde{y}^{(k)}_{\text{IC}}[n]$ and $\tilde{y}^{(k+1)}_{\text{IC}}[n]$ [13]. This asynchronous soft-demodulator outputs LLR values $z'^{(k,m)}_{\text{B}}$ which are finally interleaved and used in a SISO Hamming decoder to produce estimates $\hat{b}^{(p,k)}_{\text{B}}$ of the payload bits of user B.

B. Cancellation of the Strongest User

As previously mentioned, the proposed detector performs a hard cancellation of the symbols of user A. To this end, the interleaved LLRs $v'^{(k,m)}_{\text{A}}$ are mapped back to probabilities. The probability that user A transmitted the candidate symbol $\bar{s}$ in the k-th window is

$$p\left(s^{(k)}_{\text{A}} = \bar{s} \middle| v'^{(k,m)}_{\text{A}}\right) = \prod_{i=0}^{\text{SF}-1} \frac{e^{g_i(\bar{s}) v'^{(k,i)}_{\text{A}}}}{1 + e^{v'^{(k,i)}_{\text{A}}}}. \tag{8}$$

The detector then selects the symbol $\hat{s}^{(k)}_{\text{A}}$, which is the symbol that was the most likely to have been sent by user A

$$\hat{s}^{(k)}_{\text{A}} = \arg\max_{\bar{s}}\ p\left(s^{(k)}_{\text{A}} = \bar{s} \middle| v'^{(k,m)}_{\text{A}}\right). \tag{9}$$

To subtract the estimated symbol $\hat{s}^{(k)}_{\text{A}}$ from $\tilde{y}^{(k)}[n]$, the detector requires an estimate of its initial phase $\theta^{(k)}_{\text{A}}$. We here re-use the estimator from [13], where $\theta^{(k)}_{\text{A}}$ is estimated by retrieving the phase of the bin $\hat{s}^{(k)}_{\text{A}}$ in the DFT $Y^{(k)}$, i.e., $\hat{\theta}^{(k)}_{\text{A}} = \arctan\left(Y^{(k)}\left[\hat{s}^{(k)}_{\text{A}}\right]\right)$. The presumed contribution of user A is then cancelled from the dechirped signal $\tilde{y}^{(k)}[n]$

$$\tilde{y}^{(k)}_{\text{IC}}[n] = \tilde{y}^{(k)}[n] - \sqrt{P_{\text{A}}} e^{j\hat{\theta}^{(k)}_{\text{A}}} e^{j2\pi\hat{s}^{(k)}_{\text{A}}\frac{n}{N}}. \tag{10}$$

C. Demodulation of the Weakest User

Since the gateway is not synchronized to user B, the demodulation of this user must take into account both the STO τ and the residual CFO Δf_c. Following the dechirped signal model of (7), the symbol $\bar{s}^{(k-1)}_{\text{B}}$ of user B is split over the two windows $\tilde{y}^{(k-1)}[n]$ and $\tilde{y}^{(k)}[n]$. Therefore, to detect $\bar{s}^{(k-1)}_{\text{B}}$, the asynchronous soft-demodulator computes two partial DFTs $M^{(k-1)}_1$ and $M^{(k-1)}_2$ over the last $N - \lceil\tau\rceil$ samples of $\tilde{y}^{(k-1)}_{\text{IC}}[n]$ and the first $\lceil\tau\rceil$ samples of $\tilde{y}^{(k)}_{\text{IC}}[n]$, respectively

$$M^{(k-1)}_1\left[\bar{s}^{(k-1)}_{\text{B}}\right] = \sum_{n=\lceil\tau\rceil}^{N-1} \tilde{y}^{(k-1)}_{\text{IC}}[n] \cdot e^{-j2\pi\frac{(n-\lceil\tau\rceil)}{N}\left(\bar{s}^{(k-1)}_{\text{B}} - \tau + N\frac{\Delta f_c}{f_s}\right)} e^{-j2\pi\tau u\left[n - n^{(k-1)}_{f,2}\right]}, \tag{11}$$

$$M^{(k-1)}_2\left[\bar{s}^{(k-1)}_{\text{B}}\right] = \sum_{n=0}^{\lceil\tau\rceil-1} \tilde{y}^{(k)}_{\text{IC}}[n] \cdot e^{-j2\pi\frac{(n+N-\lceil\tau\rceil)}{N}\left(\bar{s}^{(k-1)}_{\text{B}} - \tau + N\frac{\Delta f_c}{f_s}\right)} e^{-j2\pi\tau u\left[n - n^{(k)}_{f,1}\right]}. \tag{12}$$

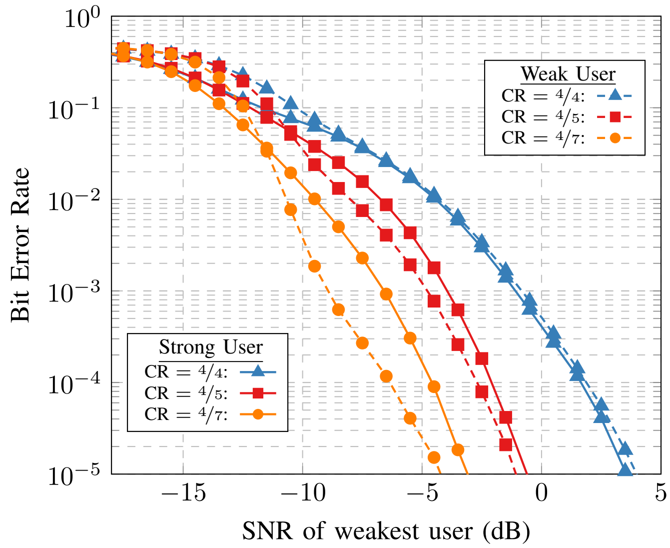

Fig. 6: BERs of both users for different coding rates, with SF $= 7$, $\tau = 16.0$, $\Delta f_c = 0$ and $\Delta P = 1.5$ dB.

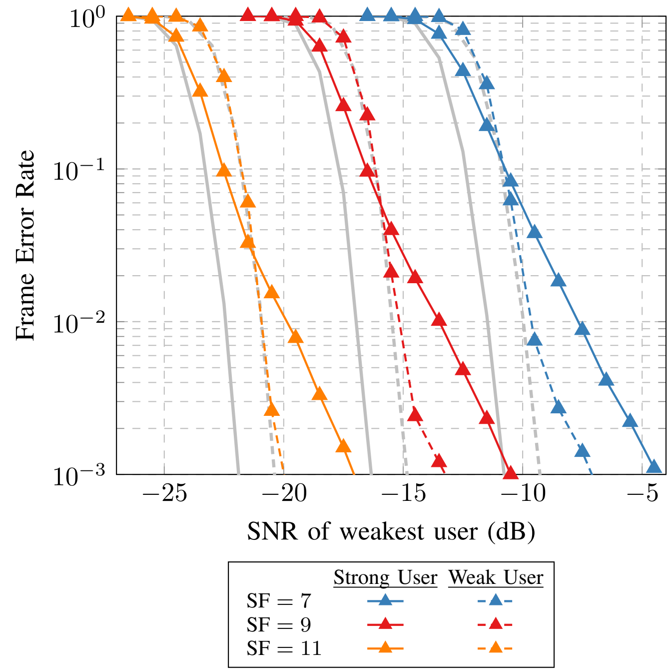

Fig. 7: Averaged FERs of both users over random values of τ and Δf_c for different spreading factors, with $\Delta P = 1.5$ dB and CR $= 4/7$. For all SFs, the colliding frames have a length of 10 information bytes. The thick gray lines show the FER of the proposed receiver in the absence of a second user.

Both partial DFTs $M_1^{(k-1)}$ and $M_2^{(k-1)}$ correct the effects of the STO and the residual CFO on the dechirped signal.

If the symbols $s_{\mathrm{A}}^{(k)}$ have correctly been cancelled in $\tilde{y}_{\mathrm{IC}}^{(k)}[n]$, it can be shown that the likelihood that user B sent the candidate symbol $\bar{s}_{\mathrm{B}}^{(k-1)}$ is given by

$$\Lambda\left(\bar{s}_{\mathrm{B}}^{(k-1)} \middle| \tilde{y}_{\mathrm{IC}}^{(k)}[n]\right) = C' I_0\left(\frac{\sqrt{P_{\mathrm{B}}}}{\sigma^2}\left|Y_{\mathrm{B}}^{(k-1)}\left[\bar{s}_{\mathrm{B}}^{(k-1)}\right]\right|\right), \quad (13)$$

where $Y_{\mathrm{B}}^{(k-1)}[\bar{s}] = M_1^{(k-1)}[\bar{s}] + M_2^{(k-1)}[\bar{s}]$ is the summation of the two partial DFTs, and C' is a constant common to all symbols of user B [13]. The LLRs at the output of the soft-demodulator are evaluated as

$$\begin{aligned} z_{\mathrm{B}}'^{(k-1,m)} = & \max_{\bar{s}:g_m(\bar{s})=1}\left[\log I_0\left(\frac{\sqrt{P_{\mathrm{B}}}}{\sigma^2}\left|Y_{\mathrm{B}}^{(k-1)}[\bar{s}]\right|\right)\right] \\ & - \max_{\bar{s}:g_m(\bar{s})=0}\left[\log I_0\left(\frac{\sqrt{P_{\mathrm{B}}}}{\sigma^2}\left|Y_{\mathrm{B}}^{(k-1)}[\bar{s}]\right|\right)\right]. \end{aligned} \quad (14)$$

IV. Performance Analysis

We now analyze the performance of our proposed two-user SIC soft-detector. We first show the beneficial effect of the Hamming code on the receiver performance, and we subsequently show general frame error rates for CR $= 4/7$ and a very small difference of received powers $\Delta P = P_{\mathrm{A}} - P_{\mathrm{B}} = 1.5$ dB.

A. Impact of Coding Rate

We study the impact of the coding rate on the decoding performance in a typical scenario with SF $= 7$. Fig. 6 shows the bit error rate (BER) of the strongest and weakest user, whose symbols are separated in time by a small STO $\tau = \frac{N}{8} = 16.0$. There is no residual CFO, i.e., $\Delta f_c = 0$.

In the absence of coding (CR $= 4/4$) and for a target BER of 10^{-4}, we observe that the strong and weak user need an SNR of 3.5 dB and 2 dB to be correctly demodulated, respectively. In a single-user scenario with the same coding rate, this BER is attained for a much lower SNR of -7 dB [1]. When enabling the coding with CR $= 4/5$, the required SNRs to achieve the same BER are -0.5 dB and -2.5 dB for the strongest and weakest user, respectively. With CR $= 4/7$, the required SNR even further decreases to -3 dB for the strongest user and -6.5 for the weakest user. We hence observe a gain of 6.5 dB for the strongest user and 8.5 dB for the weakest one when switching from CR $= 4/4$ to $4/7$, whereas in the presence of a single user, the coding only brings a gain of 2.5 dB [1].

These important SNR gains in the two-user scenario indicate that the combination of the interleaving and the Hamming coding in the BICM scheme greatly helps a SIC soft-detector to demodulate the strongest user in the presence of same-SF interference. Whereas a conventional SIC scheme without coding requires SNRs greater than zero to obtain useful error rates, our proposed receiver is capable of decoding both users with CR $= 4/7$ in the target SNR regime.

B. Averaging over STO and CFO

The previous results have been obtained for specific values of STO τ and CFO Δf_c. However, it is important to note that the performance of a multi-user LoRa receiver strongly depends on the synchronization in time and frequency of the colliding users [6], [13], [25]. While the contribution of the strongest and synchronized user to the signal after dechirping $\tilde{y}^{(k)}[n]$ is always a Kronecker delta in the frequency domain, the spectral representation of the asynchronous user symbols is, depending on the STO and CFO, modified to a bell-shaped function that spreads across several DFT bins [6]. The more the signal of the asynchronous user is spread out, the higher is the probability of correctly decoding the synchronized user.

To better assess the performance of our proposed two-user detector in practical scenarios, Fig. 7 shows the averaged probability of correctly receiving the overlapping frames of two users with $\Delta P = 1.5$ dB and CR $= 4/7$. The values of the STO τ and CFO Δf_c are uniformly distributed in the intervals $[0, N)$ and $[-\frac{f_s}{2N}, \frac{f_s}{2N}]$, respectively. The frame error rates (FERs) of the same detector in the presence of a single user at the same SNR levels (shown in gray) are also presented as baseline performance. For SF $= 7$ and a target FER of 10^{-2}, we observe that our SIC soft-receiver requires only 4 dB and 0.5 dB higher SNRs to demodulate the strongest and weakest user, respectively, compared to the corresponding single-user scenarios. We even observe that the performance of the soft-receiver improves at higher spreading factors. For SF $= 11$, the SNR loss between the two-user and single-user scenarios decreases to 2.5 dB for the strongest user, while there is no loss for the weakest user. These averaged FERs show that our proposed two-user receiver is capable of satisfactorily decoding the interfering users for all SFs, with only small SNR penalties compared to the corresponding single-user scenarios.

V. Conclusion

Multi-user receivers are a promising but challenging solution to improve the throughput of interference-limited LoRaWAN networks. In this paper, we designed a successive-interference cancellation receiver capable of decoding two colliding LoRa transmissions with the same spreading factor. The proposed receiver leverages the bit-interleaved coded modulation scheme of LoRa and performs a soft-demodulation and soft-decoding of each user. The soft-output of the decoder of the strongest user is used to reconstruct and cancel its contribution to the received signal before the decoding of the weakest user. Thanks to the efficient use of the interleaving and coding, our two-user receiver achieves useful error rates in the low SNR regime in which LoRa end-nodes operate. In future work, we will evaluate at the network level the potential benefits of deploying LoRaWAN gateways that embed the proposed two-user receiver for all spreading factors.

References

[1] T. Elshabrawy and J. Robert, "Evaluation of the BER performance of LoRa communication using BICM decoding," in *2019 IEEE 9th International Conference on Consumer Electronics*, 2019, pp. 162–167.

[2] A. Marquet, N. Montavont, and G. Z. Papadopoulos, "Investigating theoretical performance and demodulation techniques for LoRa," in *2019 IEEE 20th International Symposium on" A World of Wireless, Mobile and Multimedia Networks"(WoWMoM)*, 2019, pp. 1–6.

[3] M. C. Bor, U. Roedig, T. Voigt, and J. M. Alonso, "Do LoRa low-power wide-area networks scale?" in *Proceedings of the 19th ACM International Conference on Modeling, Analysis and Simulation of Wireless and Mobile Systems*, 2016, pp. 59–67.

[4] O. Georgiou and U. Raza, "Low power wide area network analysis: Can LoRa scale?" *IEEE Wireless Communications Letters*, vol. 6, no. 2, pp. 162–165, Apr. 2017.

[5] D. Croce, M. Gucciardo, S. Mangione, G. Santaromita, and I. Tinnirello, "Impact of LoRa imperfect orthogonality: Analysis of link-level performance," *IEEE Communications Letters*, vol. 22, no. 4, pp. 796–799, Apr. 2018.

[6] O. Afisiadis, M. Cotting, A. Burg, and A. Balatsoukas-Stimming, "On the error rate of the LoRa modulation with interference," *IEEE Transactions on Wireless Communications*, vol. 19, no. 2, pp. 1292–1304, Feb. 2020.

[7] T. Polonelli, D. Brunelli, A. Marzocchi, and L. Benini, "Slotted ALOHA on LoRaWAN - design, analysis, and deployment," *Sensors*, vol. 19, no. 4, Feb. 2019.

[8] B. Reynders, Q. Wang, P. Tuset-Peiro, X. Vilajosana, and S. Pollin, "Improving reliability and scalability of LoRaWANs through lightweight scheduling," *IEEE Internet of Things Journal*, vol. 5, no. 3, pp. 1830–1842, Jun. 2018.

[9] J. Haxhibeqiri, I. Moerman, and J. Hoebeke, "Low overhead scheduling of LoRa transmissions for improved scalability," *IEEE Internet of Things Journal*, vol. 6, no. 2, pp. 3097–3109, Apr. 2018.

[10] M. A. Ben Temim, G. Ferré, B. Laporte-Fauret, D. Dallet, B. Minger, and L. Fuché, "An enhanced receiver to decode superposed LoRa-like signals," *IEEE Internet of Things Journal*, vol. 7, no. 8, pp. 7419–7431, Aug. 2020.

[11] D. Garlisi, S. Mangione, F. Giuliano, D. Croce, G. Garbo, and I. Tinnirello, "Interference cancellation for LoRa gateways and impact on network capacity," *IEEE Access*, vol. 9, pp. 128 133–128 146, Jun. 2021.

[12] M. O. Shahid, M. Philipose, K. Chintalapudi, S. Banerjee, and B. Krishnaswamy, "Concurrent interference cancellation: decoding multi-packet collisions in LoRa," in *Proceedings of the 2021 ACM SIGCOMM 2021 Conference*, 2021, pp. 503–515.

[13] M. Xhonneux, J. Tapparel, O. Afisiadis, A. Balatsoukas-Stimming, and A. Burg, "A maximum-likelihood-based multi-user LoRa receiver implemented in GNU Radio," in *2020 54th Asilomar Conference on Signals, Systems, and Computers*, 2020, pp. 1106–1111.

[14] I. Arun and T. Venkatesh, "Order statistics based analysis of pure ALOHA in channels with multipacket reception," *IEEE Communications Letters*, vol. 17, no. 10, pp. 2012–2015, Oct. 2013.

[15] M. Chiani and A. Elzanaty, "On the LoRa modulation for IoT: Waveform properties and spectral analysis," *IEEE Internet of Things Journal*, vol. 6, no. 5, pp. 8463–8470, Oct. 2019.

[16] R. Ghanaatian, O. Afisiadis, M. Cotting, and A. Burg, "LoRa digital receiver analysis and implementation," in *ICASSP 2019-2019 IEEE International Conference on Acoustics, Speech and Signal Processing (ICASSP)*, 2019, pp. 1498–1502.

[17] O. Afisiadis, A. Burg, and A. Balatsoukas-Stimming, "Coded LoRa frame error rate analysis," in *ICC 2020 - 2020 IEEE International Conference on Communications (ICC)*, 2020, pp. 1–6.

[18] O. Seller and N. Sornin, "Low complexity, low power and long range radio receiver," Jan. 4 2018, US Patent Appl. 15/620,364.

[19] M. Xhonneux, O. Afisiadis, D. Bol, and J. Louveaux, "A low-complexity LoRa synchronization algorithm robust to sampling time offsets," *IEEE Internet of Things Journal*, 2021.

[20] J. Proakis and M. Salehi, "Optimum Receivers for AWGN Channels," in *Digital Communications*. McGraw-Hill, 2008, ch. 4, pp. 160–289.

[21] M. C. Valenti and S. Cheng, "Iterative demodulation and decoding of turbo-coded M-ary noncoherent orthogonal modulation," *IEEE Journal on Selected Areas in Communications*, vol. 23, no. 9, pp. 1739–1747, Sep. 2005.

[22] M. Ivanov, C. Häger, F. Brännström, A. G. i Amat, A. Alvarado, and E. Agrell, "On the information loss of the max-log approximation in BICM systems," *IEEE Transactions on Information Theory*, vol. 62, no. 6, pp. 3011–3025, Jun. 2016.

[23] B. Müller, M. Holters, and U. Zölzer, "Low complexity soft-input soft-output hamming decoder," in *2011 50th FITCE Congress-" ICT: Bridging an Ever Shifting Digital Divide"*, 2011, pp. 1–5.

[24] O. Afisiadis, S. Li, J. Tapparel, A. Burg, and A. Balatsoukas-Stimming, "On the advantage of coherent LoRa detection in the presence of interference," *IEEE Internet of Things Journal*, vol. 8, no. 14, pp. 11 581–11 593, Jul 2021.

[25] G. Ferré, B. Laporte-Fauret, and M. A. B. Temim, "A downlink non orthogonal multiple access for chirp spread spectrum communications," in *2020 IEEE Latin-American Conference on Communications (LATINCOM)*, 2020, pp. 1–6.